Journal of African Earth Sciences 139 (2018) 120–132

Contents lists available at ScienceDirect

Journal of African Earth Sciences

journal homepage: www.elsevier.com/locate/jafrearsci

Geochemistry and tectonic setting of the Golabad granitoid complex (SW Nain, Iran)

Mahin Mansouri Esfahani [a, *], Mahmoud Khalili [b], Zahra Alaminia [b]

[a] Department of Mining Engineering, Isfahan University of Technology, Isfahan, Iran
[b] Department of Geology, University of Isfahan, Isfahan, Iran

ARTICLE INFO

Article history:
Available online 16 December 2017

Keywords:
Golabad granitoid complex
Mineral chemistry
I- type granitoid
Urumieh–Dokhtar
Iran

ABSTRACT

The Oligo-Miocene Golabad granitoid complex intrusive into the Eocene volcanic rocks occurs in the Urumieh-Dokhtar Magmatic Arc (UDMA) in Iran. According to microscopic and chemical studies, the granitoid complex consists of three different rock types: 1) plutonic rocks comprising diorite, quartz diorite, granodiorite and granite; 2) volcanic rocks composed of basalt, andesite basalt, ± pyroxene bearing andesite and rhyolite, and 3) pyroclastic rocks. The main mineral constituents of these rocks are mostly plagioclase (oligoclase and andesine), quartz, K-feldspar, amphibole (magnesio-hornblende and actinolite-hornblende) and Mg-biotite. In addition, apatite, titanite, zircon, and opaque minerals are common accessory minerals. The studied enclaves are classified as mafic micro-granular enclaves (MME) with monzodiorite compositions. Geochemically, the rocks in this study represent medium to high-K calc-alkaline series, metaluminous and I-type nature.

Plotting, the chemical composition of plagioclase on the An-Ab-Or ternary diagram, the temperature of crystallization is estimated to range from 700 to 900 °C at a pressure of 4.5 Kbar. High TiO_2 values of biotites from the Golabad granitoid complex suggest magmatic origin and the crystallization temperature is estimated to range from 700 to 750 °C. The amphiboles according to their chemical analysis, are classified as igneous amphiboles generated in high oxygen fugacity conditions. The chemical data of the amphiboles and biotites pointed out to the I- type nature of the Golabad granitoid complex emplaced in an active continental margin subduction setting. The amphibole crystallization pressure was estimated by Al in amphibole varies from 1.09 to 2.28 Kbar. Using the calculated pressure the depth of the formation of the Golabad granitoid complex estimated from 4 to 9 Km.

1. Introduction

The collision of the Eurasian plate and the Afro-Arabian plate during the late Mesozoic and Cenozoic formed the Urumieh-Dokhtar Magmatic Arc (UDMA) (Richards and Sholeh, 2016). The UDMA along with the Sanandaj-Sirjan zone and the Zagros folded-thrust belt are the three main geological subdivisions of the Zagros orogenic belt (Alavi, 2004). The UDMA is the result of the several events including opening, subduction and closure of the Neo-Tethys Ocean. Carboniferous and Permian plutonic events in Sanandaj-Sirjan zone are considered related to the rifting and formation of the Neo-Tethys (see in Alavi, 1994). Some workers believe that the tectonic setting of UDMA is related to the continental rift (Emami, 1981; Sabzehei, 1994) whereas, others believe that its tectonic setting is associated with a subduction zone (Berberian and Berberian, 1981). Some geologists suggested that the calc-alkaline magmatism ended around 5 Ma (Late Miocene) and was replaced by alkaline magmatism associated with slab break-off (Ghasemi and Talbot, 2006; Honarmand et al., 2014). The Eocene volcanism in Iran and throughout the Middle East and the Mediterranean regions is related to the opening of back-arc basins (Kazmin et al., 1986). The beginning of most of the magmatic activities in UDMA occurred in the Eocene and continued in Middle Eocene until Plio-Quaternary formed a variety of igneous rocks (Berberian and Berberian, 1981; Ghasemi and Talbot, 2006; Torabi, 2009). Therefore, these features are the reasons for studies and investigations of this zone (UDMA) by researchers. The study area is part of the 1:250000 geological map of Nain prepared by Amidi and Alavi (1978). Mansouri Esfahani and Norbehesht (1997) studied the

* Corresponding author.
E-mail addresses: mmansouri_2001@yahoo.com, mansoori@cc.iut.ac.ir (M. Mansouri Esfahani).

https://doi.org/10.1016/j.jafrearsci.2017.12.004
1464-343X/

geology and petrology of the granitoid intrusions of the southwest of the Nain area. Amidi (1975) studied stratigraphy, petrology and geochemistry of Surk-Nain-Natanz and believed that the mainrocks belong to Pliocene volcanism. Javanmardi and Davoudian (2009) recognised the pumpellyite-prehnite- quartz rock assemblages as an important metamorphic facies in the north east of the Kohpaeh volcanic rocks (east of Isfahan city). Jahanbakhsh (2014) carried out geochemical and petrological studies on the Golabad intrusive body in the southwest of Nain. He believed that this intrusive body is I-type and shows calc-alkaline nature.

The aim of this study is to determine the geochemistry, tectonic setting and the role of magma mixing in the generation and evolution of the Golabad granitoids in the Nain area. The research is supported by petrographical and geochemistry observations as well as the mineral chemistry analysis of plagioclase, amphibole and biotite.

2. Geological setting

The Golabad granitoid complex is located about 100 Km east of Isfahan, 40 Km southwest of Nain city and geologically it lies in the central part of the UDMA (Fig. 1A). The area is cut by the Qom-Zefreh and Dehshir-Baft faults (Fig. 1B). These faults trend in an NE-SW direction. Several outcrops of plutonic rocks are related to these faults or other subsidiary faults associated with these two main faults (Fig. 1A).

The oldest sedimentary rocks in the eastern corner of the studied area present nearly small outcrops of conglomerate layers with the Paleocene age. The Eocene volcanic rocks which cross-cutting by the Oligo-Miocene granitoid body, consist of basalt, andesite-basalt, ± pyroxene bearing andesite, trachyte, dacite and rhyolite (Fig. 1C). The Eocene meta-andesite and meta-basaltic rocks observed in proximity to the Golabad granitoid complex. These rocks are related to the granitoid intrusion and development of a contact metamorphism with a low-grade albite-epidote hornfels facies (Fig. 2A). Most of the volcanic rocks are located in the northern and eastern parts of the plutonic rocks. The basalt outcrops are mostly located in the northern portion of the plutonic rocks which show fine-grained and grey to dark green in colour. While rhyolitic rocks mostly display a dome shape in the west and the southwest of the Golabad granitoid complex. The components of the pyroclastic rocks are widely dominated by rhyolite, dacite and andesite which mostly seen in northern and southern part of the studied area. They mostly trend in an NW-direction. Numerous diabasic and aplite dykes crosscut the pyroclastics as well as the Golabad granitoid complex (Fig. 2B and C). The Pliocene conglomerates with intercalation of sandstone layers are the main sedimentary rocks of the studied area. Microgranular mafic enclaves

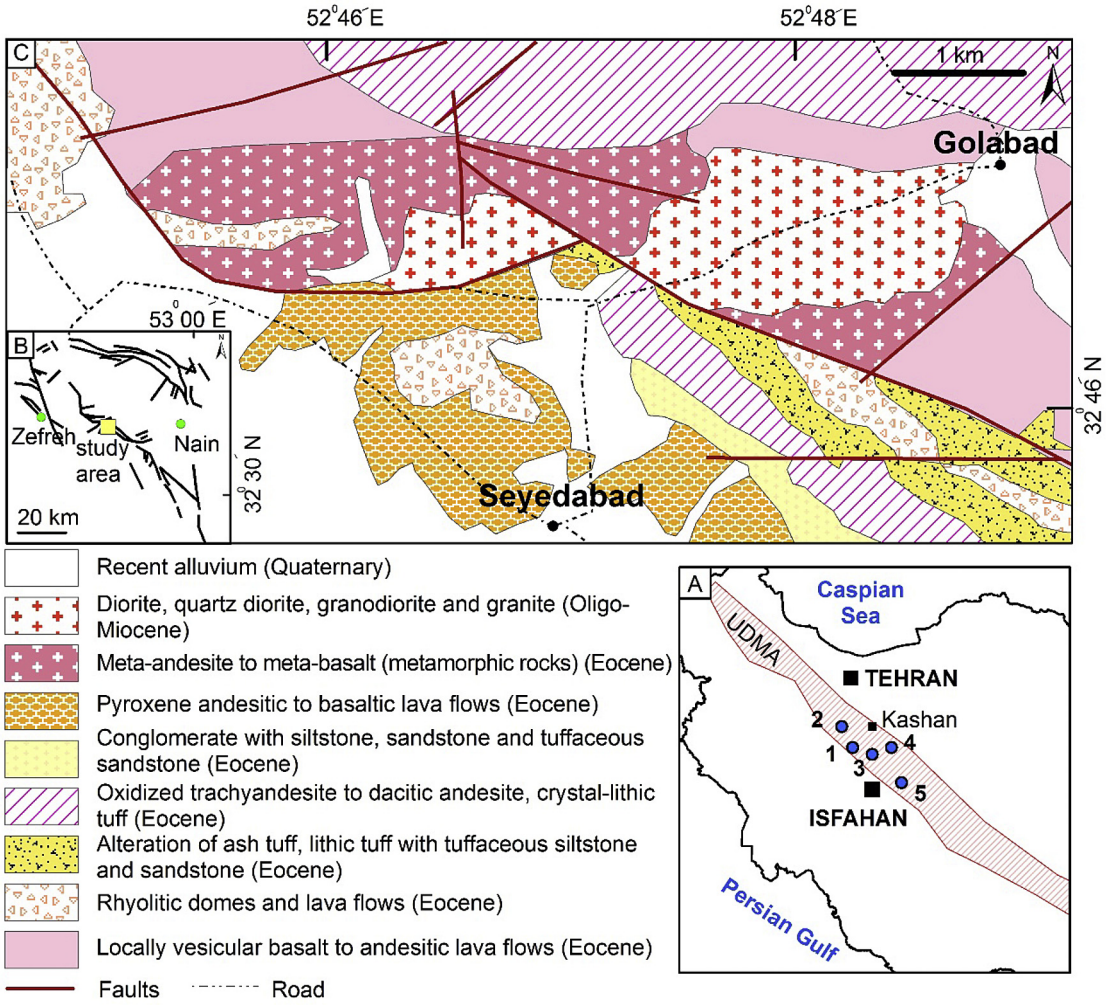

Fig. 1. (A) The geological situation of the Urumieh-Dokhtar magmatic arc (UDMA); the location of granitoid complexes is shown as: 1-Nabar, 2-Niyasar, 3-Ghohroud, 4-Natanz and 5-Golabad; (B) The major faults in the Golabad granitoid area; (C) Simplified geological map of the studied area (modified after Emami, 1981).

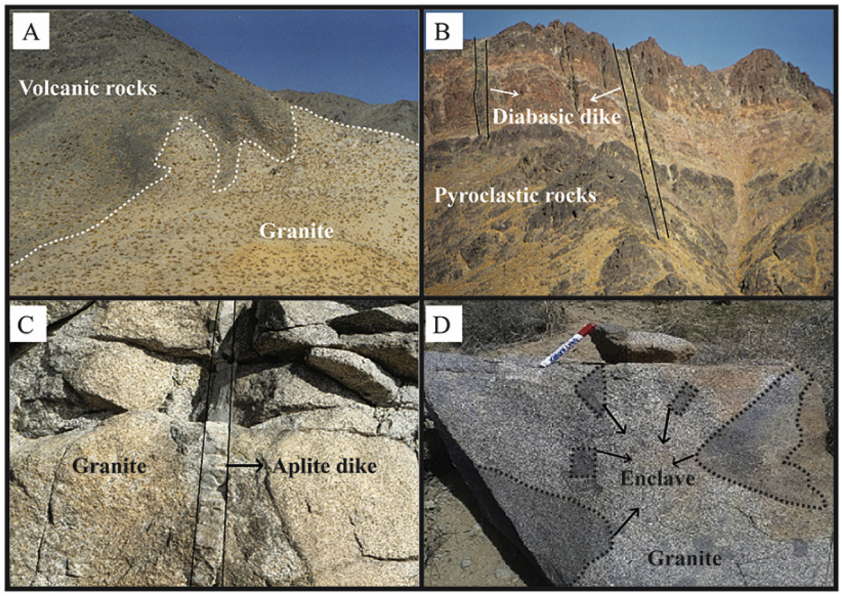

Fig. 2. (A) The Eocene meta-andesite and meta-basaltic rocks in the vicinity of the granitoid body; (B) Diabasic dike crosscutting the pyroclastic rocks; (C) Aplite dike crosscutting the granitoid rocks; (D) Microgranular mafic enclaves (MME) with sharp contact.

(MME) with elliptical shape display sharp contact and sometimes transitional border with the contiguous host rocks (Fig. 2D).

3. Petrography

Based on field investigations and petrographical observations, the Golabad granitoid complex classified into three type of rocks: 1) plutonic rocks consist of diorite, quartz diorite, granodiorite and granite; 2) volcanic rocks present with a component of basalt, andesite basalt, ± pyroxene bearing andesite and rhyolite. 3) pyroclastic rocks. Also, the enclaves mostly display as microgranular mafic enclaves with monzodiorite composition.

3.1. Plutonic rocks

3.1.1. Diorite and quartz diorite

The main minerals of the studied diorites and quartz diorites are plagioclase, amphibole, biotite, ±quartz with minor minerals of K-feldspar, and opaque. Calcite, chlorite, epidote and sericite are common alteration minerals. Euhedral to subhedral plagioclase displays with polysynthetic twin and oscillatory zoning. Some of the plagioclases altered to epidote and sericite by the sasuaritization process. Subhedral to anhedral amphibole occurs as primary and secondary minerals with yellow to brownish-green colours (Fig. 3A). Sometimes, the amphiboles during of the retrograde metamorphism process formed the secondary biotites (Fig. 3A). Fine to medium-grained and euhedral to subhedral biotites occur as primary and secondary minerals. Formation of the epidote during the alteration of the biotite to chlorite is related to the thermal metamorphism which often occurs on the margin of the Golabad granitoid complex (Deer et al., 1992) (Fig. 3B). Medium to coarse-grained quartz usually shows interstitial texture. Fine-grained and anhedral K-feldspar in the rocks is a minor mineral. Pyroxene is observed in very small amounts in some of the rocks. The pyroxenes have mostly been altered to chlorite, epidote and calcite by uralitization process. The presence of titanite as an accessory mineral in most of the studied rocks as well as associated minerals such as magnetite, quartz and amphibole is evidence for high oxygen fugacity (Wones, 1989).

3.2. Granodiorite

Granodiorites and granite are medium-grained in texture and cream to green in colour. They contain plagioclase, quartz and K-feldspar as the main minerals and amphibole, biotite, zircon and apatite as minor minerals. Plagioclase usually is represented by polysynthetic twins and sometimes it is zoned. Quartz shows anhedral form with medium to fine grains. There are also coarser quartz grains that surrounds the plagioclase, hornblende and biotite in poikilitic texture. Didier (1973) believed that this feature in quartz is due to crystallization of a more felsic melt or hydrous melting which has occurred after the formation of the fine crystals of plagioclase, hornblende and biotite in the mafic magmatic system during the development and evolution of the hybrid system. Fine to medium-grained and anhedral K-feldspar sometimes shows intergrowth in micro-perthite texture often altered to sericite. Euhedral to subhedral amphiboles are present in various sizes. Subhedral to anhedral and sometimes medium-grained biotite occurred yellow to brown in colour. Due to the effects of the deformation biotites are observed with bend forms, as well as mechanical twinning in some of the biotites, suggested tectonic deformation (Fig. 3C). Alteration by thermal metamorphism in some of the biotites led to the formation of repidolite and released titanite along the cleavages of the biotites (Fig. 3D). Apatite occurs as a minor mineral in these rocks and shows needle forms which may represent abrupt cooling of the melt due to the magma mixing process (Didier and Barbarin, 1991; Best, 2003).

3.3. Volcanic and pyroclastic rocks

The volcanic and pyroclastic rocks surround the Golabad granitoid outcrop and are dominated by basalt, andesite basalt, ± pyroxene bearing andesite and rhyolite as well as pyroclastic rocks consisting of crystal lithic tuff and ash tuff. The plagioclases in the basalts and andesites show microlithic shapes (lath) and well-formed triangular habits surrounded by amphiboles and biotite

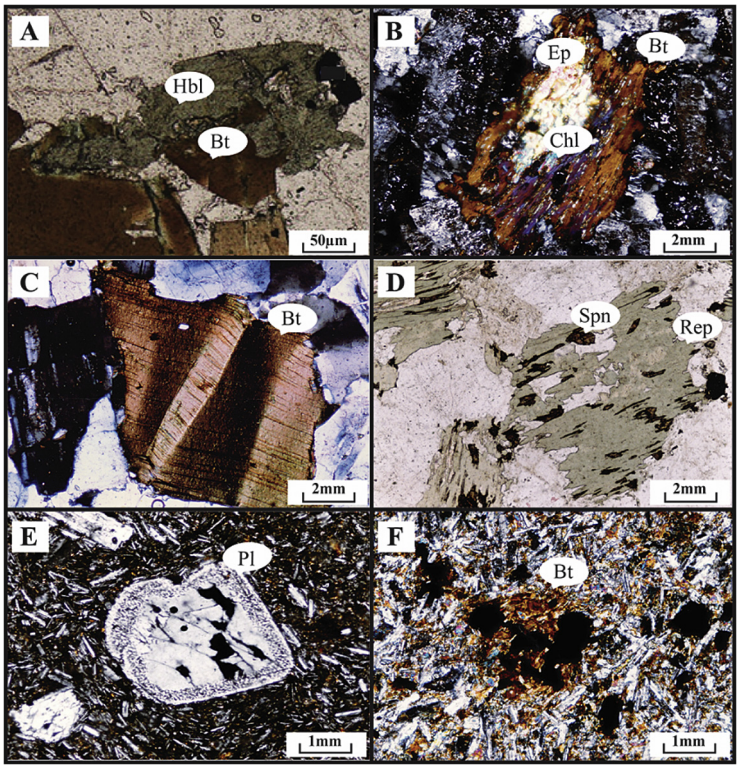

Fig. 3. Photomicrographs of the Golabad granitoid body: (A) Subhedral to anhedral habit in the amphiboles, formation of the secondary biotite at the expense of amphibole; (B) Crystallization of the epidote during thermal alteration of the chlorite; (C) Mechanical twin in the biotites; (D) Repidolite (Rep) released titanite along the cleavages of the biotites; (E) Dusty zone in the plagioclase pointing to magma mixing process; (F) Assemblages of the biotite flakes within the basalts. Mineral abbreviations were taken from Whitney and Evans (2010).

forming an intergranular texture. The presence of the plagioclase with a dusty zone texture in these rocks by suggests magma mixing process (Vernon, 1990) (Fig. 3E). Also, some of the plagioclases are rounded in shape and have corroded margins which can result from magma mixing processes (Fig. 3E) (Zorpi et al., 1989; Shelley, 1993). Amphiboles occur as phenocrysts as well as fine-grains in the groundmass of the basalt and andesite. They exhibit euhedral to subhedral habit and are green to brown in colour as well as altered to chlorite, epidote and calcite. Assemblages of the biotite flakes within the basalts can be used as evidence of magma mixing processes (Vernon, 1990) (Fig. 3F). The rhyolites of the area are distinguished by quartz, K-feldspar (sanidine), plagioclase and biotite phenocrysts in a fine-grained matrix consisting of quartz, K-feldspar, plagioclase, biotite and volcanic glass. Quartz grains are observed in medium size and show chemical corrosion in gulf form. Subhedral to anhedral K-feldspar are altered to sericite and sometimes show Carlsbad twinning. Euhedral to subhedral and fine to coarse-grained plagioclase occur as zoned crystals, rarely altered to sericite, epidote and calcite. Euhedral to subhedral biotite is the only mafic mineral.

3.4. Mafic micro-granular enclaves

Mafic microgranular enclaves (MME) predominantly consist of mafic mineral assemblages, are relatively fine-grained and commonly exhibit ellipsoidal shapes (i.e., Vernon, 1990; Barbarin, 2005). The above authors believe that the enclaves originate by hybridism processes which form globules of more mafic magma that are quenched in the more felsic magma of the host granitoid pluton.

The micro-granular enclaves are 10–40 cm in size and rounded to ellipsoidal in shape and have sharp margins with the host granitoids. The MME from this area are monzodioritic in composition. The essential minerals in the MME's are plagioclase, hornblende, biotite and K-feldspar. Plagioclases display a coarse-grained and sometimes formed as fine-grained in lath shape. They occur as euhedral to subhedral grains with corrosion rims and also characterized by albite twins. Euhedral to subhedral and fine to medium amphiboles are sometimes altered to chlorite, epidote and iron oxide. Euhedral to anhedral and often fine to medium in texture biotites show yellow to brownish red pleochroism and are sometimes altered to chlorite. The predominant textures of enclaves observed are micro-granular, porphyroid, poikilitic and consertal.

4. Analytical method

The petrographic study was performed on over 65 thin sections. Ten (10) fresh granitoid rock samples were selected for the analysis of major and trace elements. Four (4) samples were analyzed by ICP-MS methods by the Zarazma Mineral Studies Company in Tehran- Iran, and the rest of the samples were analyzed by X-ray fluorescence (XRF) using a Philips PW 2400 at the Dallas Southern University in the USA (Table 1). Eighteen (18), fifteen (15) and twelve (12) plagioclase, amphibole and biotite minerals respectively were analyzed by electron microprobe analysis (EMPA) at the Iranian Mineral Processing Research Center (IMPRC) (Tables 2–5). Analytical conditions were wavelength dispersive spectroscopy (WDS) utilising a Cameca SX-100 microprobe operated at 20 kV, accelerating voltage, 25-nA beam current and 3-μm defocused spot size.

Table 1
Major and trace elements analyses by ICP-MS and XRF methods for representative granitoid samples from the Golabad and Natanz granitoid complexes.

Rock types	Granite[b]	Granodiorite			Diorite				Monzodiorite (Enclaves)		
Sample No.	GT1	GR1	GR2	GR3	GD1[a]	GD2[a]	GD3[a]	GD4	GE1[a]	GE2[a]	GE3[a]
SiO_2(wt%)	69.96	64.84	65.49	66.14	56.68	58.35	60.02	61.49	50.12	52.05	55.25
TiO_2	0.37	1.41	0.39	0.38	0.94	0.85	0.75	0.49	0.63	0.78	0.69
Al_2O_3	14.85	17.33	17.14	16.96	16.35	16.61	16.87	17.94	19.67	19.73	19.33
Fe_2O_3	1.75	1.50	1.46	1.47	3.62	3.30	2.98	1.96	3.5	2.81	2.68
FeO	1.54	2.23	2.21	2.18	4.3	3.80	3.29	2.94	5.08	4.42	4.02
MnO	0.07	0.08	0.08	0.07	0.16	0.15	0.14	0.12	0.42	0.23	0.21
MgO	1.07	1.94	1.87	1.80	3.86	3.45	3.03	2.44	4.79	3.82	4.07
CaO	3.16	4.46	4.38	4.30	6.99	6.31	5.62	5.16	6.66	6.84	6.25
Na_2O	3.82	3.94	4.01	4.08	2.98	3.30	3.61	3.33	4.25	4.63	4.54
K2O	3.2	2.54	2.22	1.90	2.46	2.46	2.46	3.18	2.20	2.21	1.80
P_2O_5	0.07	0.19	0.21	0.17	0.60	0.49	0.37	0.25	0.28	0.32	0.32
LOI	0.14	0.54	0.54	0.55	1.08	0.98	0.88	0.68	1.72	1.56	0.84
Total	100.00	100.00	100	100.00	100.1	100.06	100.02	100.00	99.32	99.40	100.53
$Na_2O + K_2O$	7.03	6.48	6.23	5.98	5.44	5.45	6.07	6.51	6.45	6.84	6.34
K_2O/Na_2O	0.83	0.64	0.55	0.46	0.82	0.74	0.68	0.95	0.51	0.47	0.39
A/NK	1.52	1.87	1.90	1.93	2.16	2.05	1.96	2.01	1.86	1.97	2.06
A/CNK	0.95	0.99	0.01	1.02	0.80	0.84	0.89	0.98	0.81	0.97	0.81
Ba (ppm)	657.11	603	302	563	865	907	949	657	410	500	320
Rb	94.51[a]	67	33.55	55	52	55.5	59	73	67.3	62.5	71.2
Sr	193[a]	325	444	324	439	417.5	396	333	265	280	250
Zr	152 [a]	85	96	104	127	63.5	154	95	83	76	84
Zn	39	44	51	41	94	88.5	83	52	80	90	70
Cu	nd	33	55	58	61	52.5	44	23	21	25	17
Ni	15	14	13	13	11	10.5	10	12	9	9	9
V	54.2	79	44	77	184	129	74	91	85	100	70
Co	6.71	10	11.5	9.4	29	25.5	22	9.8	10	13	7
Y	17.49	10.1	8.10	9.2	22.8	11.40	15.8	16.1	30	48	12
Nb	6.19[a]	6.4	3.56	6.5	3.00	3.90	4.80	8.1	3.90	4.8	3
Th	17.25	6.8	8	6.69	3.69	1.84	7.3	9.84	7.64	3.49	3.69
U	4.41	1.6	4.15	1.2	0.8	1.2	1.60	2.7	1.8	2.3	1.5
La	25.63	16	8.20	1.2	10	9	9	12	29	25	27
Ce	45.73[a]	32	22	12	19	20.50	21	26	22	20	21
Rb/Sr	0.11	0.20	0.07	0.17	0.11	0.13	0.14	0.21	0.25	0.22	0.28
Th/U	3.90	4.25	1.93	5.60	4.61	1.53	4.56	3.64	4.24	1.52	2.46
Y + Nb	23.68	16.50	11.66	15.70	25.80	15.30	20.70	24.20	33.90	52.80	15.00

nd = not determined.
[a] Analyzed by XRF method.
[b] The chemical analyzes data is from Honarmand et al. (2010).

Table 2
Rare earth elements compositions of the Golabad and Natanz granitoid complexes.

Rock type	Granite[a]	Granodiorite			Diorite
Sample No	GT1	GR1	GR2	GR3	GD4
La	25.63	16	14.2	12	12
Ce	45.71	35	32	37	26
Pr	4.82	4.1	3.76	3.44	3.91
Nd	16.79	11.1	9.92	8.7	11.9
Sm	3.31	2.59	2.46	2.34	3.28
Eu	0.77	0.92	0.89	0.84	1
Gd	2.99	2.04	1.97	1.85	2.47
Tb	0.46	0.34	0.36	0.31	0.44
Dy	2.71	1.8	1.65	1.58	2.73
Ho	0.62	nd	nd	nd	nd
Er	1.89	1.2	1.25	1.18	1.65
Tm	0.31	0.19	0.19	0.20	0.31
Yb	2.12	1.1	1.06	1.00	1.6
Lu	0.34	0.18	0.17	0.18	0.25
Eu/Eu[b]	0.75	1.22	1.06	1.23	1.07
La/Yb	12.09	8.20	12.00	14.54	7.5
Th/Yb	8.14	8.00	6.69	6.18	6.15

nd = not determined.
Rare earth elements are normalized by data from Boynton (1984).
[a] The chemical analyzes data are from Honarmand et al. (2010).
[b] Analyzed by ICP-MS method.

5. Whole rocks geochemistry

The results of major and trace elements analyse of the granitoid samples from the Golabad granitoid complex are in Tables 1 and 2. Due to lack of chemical analysis from granitic rocks, sample (GT1) from the Oligo-Miocene Natanz granitoid complex was taken (Honarmand et al., 2010) and plotted on the whole rock diagrams. According to chemical characteristics, the intrusive rocks of the studied area and those from Natanz are determined into diorite, granodiorite, granite, and monzodiorite which occur as enclaves (Fig. 4). The studied rock samples represent medium to high-K calc-alkaline series on K_2O versus SiO_2 diagram (Peccerillo and Taylor, 1976) (Fig. 5). According to the alumina saturated Index (ASI = 0.80–1.02) values of the Golabad and Natanz granitoid rocks on the A/NK ratio versus A/NKC diagram (Maniar and Piccoli, 1989) display metaluminous features and are I-type in nature (Fig. 6).

6. Mineral chemistry

6.1. Plagioclase

The composition of plagioclase depends on magmatic gas, in addition to the composition and temperature of the magma, also with the increase of magmatic-water, the amount of anorthite in plagioclaseis also increased (Hattory and Sato, 1996). Representative chemical analyses of the plagioclase composite data from the

Table 3
Representative electron microprobe analyses of feldspar from the Golabad granitoid complex.

Rock types	Granodiorite						Diorite						Monzodiorite (Enclaves)					
Sample No.	P-1	P-2	P-3	P-4	P-5	P-6	P-7	P-8	P-9	P-10	P-11	P-12	P-13	P-14	P-15	Or-1	Or-2	Or-2
SiO_2	55.84	57.66	57.61	63.08	54.34	59.52	61.66	55.71	55.97	57.73	59.82	56.9	57.61	56.25	58.97	64.66	65.02	64.14
TiO_2	0.01	0.02	0.03	0.01	0.00	0.03	0.02	0.01	0.03	00.00	00.00	00.00	0.00	0.00	0.00	0.02	00.00	0.03
Al_2O_3	26.22	27.20	26.20	22.83	28.09	23.76	22.69	25.78	24.89	23.65	22.83	22.85	27.16	27.24	25.76	18.12	18.22	18.40
FeO*	0.20	0.14	0.19	0.11	0.16	0.11	0.15	0.13	0.12	0.15	0.08	0.35	0.15	0.19	0.18	0.08	0.08	0.07
MnO	0.02	0.00	0.00	0.00	0.00	0.01	0.01	0.01	00.00	00.00	00.00	00.00	0.00	0.01	0.00	00.00	00.00	00.00
MgO	0.00	0.00	0.00	0.00	0.00	0.00	0.01	00.00	00.00	0.04	0.07	0.04	0.01	0.00	0.00	00.00	00.00	00.00
CaO	8.59	9.11	8.31	4.61	10.65	5.02	3.69	8.85	8.54	5.79	6.52	8.91	9.45	9.86	7.93	0.02	0.02	0.05
Na_2O	7.07	6.49	7.35	9.63	6.20	9.43	10.40	7.76	7.81	10.93	8.75	7.95	6.60	6.25	7.57	1.25	1.16	1.19
K_2O	0.20	0.21	0.19	0.37	0.12	0.24	0.00	00.00	00.00	00.00	00.00	00.00	0.15	0.20	0.24	16.88	17.02	17.06
Total	98.15	100.83	99.88	100.64	99.56	98.12	98.63	98.25	97.36	98.29	98.07	97.00	101.13	100.01	100.65	101.03	101.52	100.94
Structural formula based on 8 Oxygens																		
Si	2.56	2.57	2.59	2.79	2.47	2.71′	2.78	2.56	2.59	2.65	2.72	2.65	2.56	2.53	2.63	2.98	2.98	2.97
Ti	0.00	0.00	0.00	0.00	0.00	0.00	0.00	0.00	0.00	0.00	0.00	0.00	0.00	0.00	0.00	0.00	0.00	0.00
Al	1.42	1.43	1.39	1.19	1.50	1.27	1.20	1.39	1.36	1.28	1.22	1.25	1.42	1.44	1.35	0.98	0.98	1.00
Fe^{2+}	0.00	0.00	0.00	0.00	0.00	0.00	0.00	0.00	0.00	0.00	0.00	0.00	0.00	0.00	0.00	0.00	0.00	0.00
Fe^{3+}	0.01	0.00	0.01	0.00	0.01	0.00	0.01	0.00	0.00	0.01	0.00	0.01	0.01	0.01	0.01	0.00	0.00	0.00
Mn	0.00	0.00	0.00	0.00	0.00	0.00	0.00	0.00	0.00	0.00	0.00	0.00	0.00	0.00	0.00	0.00	0.00	0.00
Mg	0.00	0.00	0.00	0.00	0.00	0.00	0.00	0.00	0.00	0.00	0.00	0.00	0.00	0.00	0.00	0.00	0.00	0.00
Ca	0.42	0.43	0.40	0.22	0.52	0.24	0.18	0.44	0.42	0.28	0.32	0.44	0.45	0.48	0.38	0.00	0.00	0.00
Na	0.63	0.56	0.64	0.82	0.55	0.83	0.91	0.69	0.70	0.97	0.77	0.72	0.60	0.55	0.65	0.11	0.10	0.11
K	0.01	0.01	0.01	0.021	0.01	0.01	0.00	0.00	0.00	0.00	0.00	0.00	0.01	0.01	0.01	0.99	0.91	1.01
Ba	0.00	0.00	0.00	0.00	0.00	0.00	0.00	0.00	0.00	0.00	0.00	0.00	0.00	0.00	0.00	0.00	0.00	0.00
Cations	5.05	5.00	5.04	5.04	5.06	5.08	5.08	5.07	5.19	5.07	5.03	5.07	5.05	5.02	5.03	5.06	5.07	5.09
Ab	59.20	55.60	60.90	77.50	51.00	76.30	83.60	61.30	62.30	77.30	70.90	61.70	55.40	52.90	62.50	10.10	9.40	9.60
An	39.70	43.20	38.10	20.50	48.40	22.50	16.40	38.70	37.70	22.70	29.10	38.30	43.80	46.10	36.10	0.10	0.10	0.20
Or	1.10	1.20	1.00	2.00	0.70	1.30	0.00	0.00	0.00	0.00	0.00	0.00	0.90	1.10	1.30	89.80	90.50	90.20

Table 4
Representative electron microprobe analyses of the amphibole from the Golabad granitoid complex.

Rock types	Granodiorite						Diorite						Monzodiorite (Enclaves)		
Sample No.	G-1	G-2	G-3	G-4	G-5	G-6	D-1	D-2	D-3	D-4	D-5	D-6	E-1	E-2	E-3
SiO_2	50.92	51.15	49.01	52.58	52.55	51.52	51.39	52.38	51.15	49.01	52.58	52.55	51.52	51.39	50.61
TiO_2	0.86	0.60	0.85	0.82	0.38	0.68	0.69	0.48	0.60	0.85	0.82	0.38	0.68	0.69	0.52
Al_2O_3	4.60	3.94	4.45	4.90	5.18	3.89	4.85	3.62	3.94	4.45	4.90	5.18	3.89	4.85	4.83
Cr_2O_3	0.01	0.00	0.00	0.01	0.02	0.00	0.00	0.00	0.00	0.00	0.01	0.02	0.00	0.00	0.01
FeO*	12.79	12.60	13.04	12.33	12.05	12.23	13.08	12.62	12.60	13.04	12.33	12.05	12.23	13.08	13.72
MnO	0.78	0.79	0.87	0.61	0.59	0.78	0.68	0.70	0.79	0.87	0.61	0.59	0.78	0.68	0.67
MgO	15.76	16.42	16.08	16.27	17.35	16.47	15.72	16.03	16.42	16.08	16.27	17.35	16.47	15.72	15.96
CaO	11.69	11.75	11.46	11.79	12.25	11.70	10.63	11.70	11.75	11.46	11.79	12.25	11.70	10.63	11.28
Na_2O	0.99	0.75	0.85	1.01	0.84	0.87	1.32	0.69	0.75	0.85	1.01	0.84	0.87	1.32	1.13
K_2O	0.30	0.36	0.39	0.43	0.31	0.33	0.25	0.25	0.36	0.39	0.43	0.31	0.33	0.25	0.44
Total	98.69	98.36	97.00	100.74	101.50	98.47	98.61	98.47	98.36	97.00	100.74	101.50	98.47	98.61	99.16
Structural formula based on 23 Oxygens															
Si	7.25	7.31	7.16	7.31	7.20	7.34	7.30	7.44	7.25	7.31	7.16	7.31	7.200	7.34	7.20
Ti	0.09	0.06	0.09	0.09	0.04	0.07	0.07	0.05	0.09	0.06	0.09	0.09	0.04	0.07	0.06
Al^{IV}	0.77	0.66	0.77	0.73	0.84	0.65	0.78	0.60	0.77	0.66	0.77	0.73	0.84	0.65	0.80
Al^{VI}	0.00	0.00	0.00	0.06	0.00	0.00	0.02	0.00	0.00	0.00	0.00	0.06	0.00	0.00	0.00
Cr	0.00	0.00	0.00	0.00	0.00	0.00	0.00	0.00	0.00	0.00	0.00	0.00	0.00	0.00	0.00
Fe^{2+}	1.04	1.09	1.24	1.03	0.70	1.07	1.09	1.06	1.04	1.09	1.24	1.03	0.70	1.07	1.14
Fe^{3+}	0.49	0.41	0.36	0.40	0.68	0.39	0.46	0.44	0.49	0.41	0.36	0.40	0.68	0.39	0.49
Mn	0.09	0.10	0.11	0.07	0.07	0.09	0.08	0.08	0.09	0.10	0.11	0.07	0.07	0.09	0.08
Mg	3.35	3.46	3.50	3.37	3.54	3.50	3.33	3.40	3.35	3.46	3.50	3.37	3.54	3.50	3.39
Ca	1.78	1.80	1.79	1.80	1.80	1.79	1.62	1.78	1.78	1.80	1.79	1.80	1.80	1.79	1.72
Na	0.27	0.21	0.24	0.22	0.22	0.24	0.36	0.19	0.27	0.21	0.24	0.22	0.22	0.24	0.31
K	0.05	0.07	0.07	0.05	0.05	0.06	0.04	0.04	0.05	0.07	0.07	0.05	0.05	0.06	0.08
Cations	15.18	15.17	15.33	15.13	15.14	15.20	15.15	15.08	15.18	15.17	15.33	15.13	15.14	15.20	15.27

Golabad granitoid complex are reported in Table 3. On the Or-Ab-An triangle diagram (Deer et al., 1992) showed that the plagioclases compositions of the diorite, granodiorite and monzodiorite (enclaves) rocks are oligoclase to andesine domain (Fig. 7A). The plagioclases of the granodiorite and diorites rocks from the area display oscillatory zoning which can be an evidence of magma mixing (Shelley, 1993) (Fig. 7B).

6.2. Amphibole

Representative analyses of amphibole from the studied area are presented in Table 3. The amphibole data on BNa vs. BCa + BNa diagram (Leake et al., 1997) display that these phases are member of the calcic group (Fig. 8A). Compositionally, the amphiboles are magnesio-hornblende and actinolite-hornblende in the diorite and

Table 5
Representative electron microprobe analyses of the biotites in the granodiorite samples from the Golabad granitoid complex.

Samples No.	B-1	B-2	B-3	B-4	B-5	B-6	B-7	B-8	B-9
SiO_2	36.79	36.89	38.06	36.79	36.70	38.11	38.31	38.00	37.76
TiO_2	3.71	3.21	3.94	3.72	3.82	3.71	3.87	3.66	3.67
Al_2O_3	13.63	13.55	13.88	13.74	13.72	14.13	13.79	14.24	13.69
FeO*	15.67	15.84	18.25	18.69	18.57	18.83	17.65	17.95	17.52
MnO	0.46	0.35	0.43	0.53	0.53	0.52	0.44	0.42	0.41
MgO	13.84	12.88	13.57	12.84	12.74	13.03	13.95	13.89	13.86
CaO	0.03	0.02	0.03	0.09	0.05	0.06	0.02	0.04	0.02
Na_2O	0.00	0.21	0.17	0.22	0.21	0.21	0.21	0.20	0.31
K_2O	9.85	9.83	10.71	10.61	10.68	10.45	10.60	10.51	10.49
Total	93.99	92.78	99.04	97.27	97.04	99.05	98.84	98.91	97.73
Structural formula based on 22 Oxygens									
Si	5.63	5.72	5.60	5.55	5.55	5.61	5.63	5.58	5.61
Ti	0.43	0.37	0.44	0.42	0.43	0.41	0.43	0.40	0.41
Al^{IV}	2.37	2.28	2.40	2.44	2.44	2.39	2.37	2.42	2.39
Al^{VI}	0.09	0.20	0.01	0.00	0.00	0.06	0.01	0.05	0.01
Fe^{2+}	2.00	2.05	2.24	2.36	2.35	2.32	2.17	2.20	2.18
Fe^{3+}	0.00	0.00	0.00	0.00	0.00	0.00	0.00	0.00	0.00
Mn	0.06	0.05	0.05	0.07	0.07	0.06	0.05	0.05	0.05
Mg	3.16	2.98	2.98	2.89	2.87	2.86	3.05	3.04	3.07
Ca	0.00	0.00	0.00	0.01	0.09	0.01	0.00	0.07	0.00
Na	0.00	0.06	0.05	0.06	0.06	0.06	0.06	0.06	0.09
K	1.92	1.94	2.01	2.04	2.06	1.96	1.99	1.97	1.99
Cations	15.66	15.65	15.78	15.84	15.92	15.74	15.76	15.84	15.80

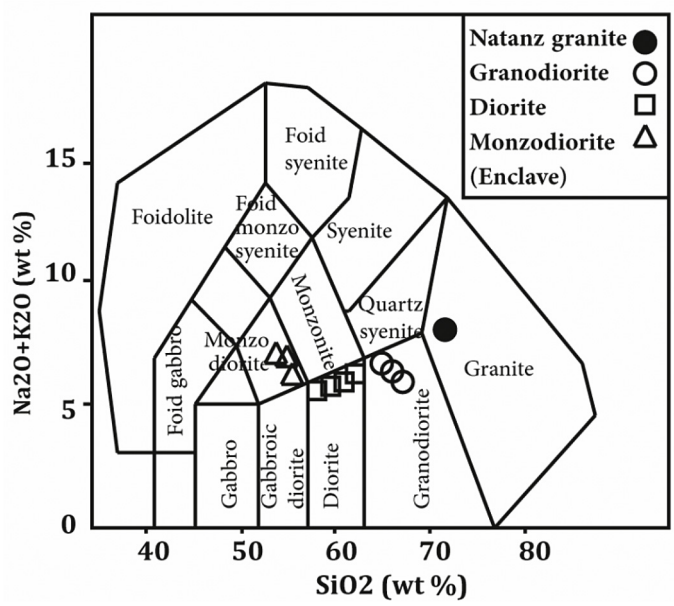

Fig. 4. Classification of the rock samples of the Golabad and Natanz granitoid complex on $Na_2O + K_2O$ vs. SiO_2 diagram (after Middlemost, 1994).

granodiorite as well as in monzodioritic enclaves (Leake et al., 1997) (Fig. 8B). Leake et al. (1997) believe that Al^{IV} variation in calcic amphiboles is related to Ti content, thus, the Al^{IV} values decrease with increasing the amount of Ti. But for some events, such as mixing, alteration and contamination processes, the trend is completely reverse.

Amphiboles from igneous and metamorphic processes are classified by Al^{IV} versus Al^{VI} diagram (Fleet and Barnett, 1978). The amphiboles from the rocks are igneous nature, originated by magmatic process (Fig. 8C). Moreover, the trend of Ti/Al^{IV} values from the amphiboles on the Ti versus Al ^{IV} diagram shows the involvement of the magma mixing and contamination role in the evolution of the studied rocks (Fig. 8D).

6.3. Biotite

Several studies have been demonstrated the application of biotite composition as a valuable guide to granite petrogenesis (e.g., Finch et al., 1995). In addition, the classical experimental works of Wones and Eugster (1965) clearly display that biotite as a valuable indicator of redox conditions in granitic magmas. Representative analyses of biotite from the Golabad granitoid complex are listed in Table 5. On the Mg-(Fe^{2+}+Mn)-(Al^{VI} + Fe^{3+}+Ti) ternary diagram (Foster, 1960), the biotites from the area are classified as Mg-biotite (Fig. 9A). And, except for the biotites from the enclaves, which are equilibrated primary phases, all others are magmatic biotite (Nachit et al., 2005) (Fig. 9B).

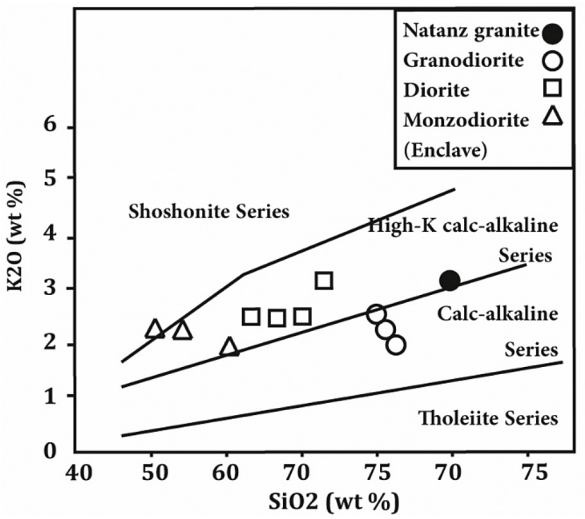

Fig. 5. K_2O versus SiO_2 diagram indicating medium to high-K calc-alkaline series for the studied rocks (after Peccerillo and Taylor, 1976).

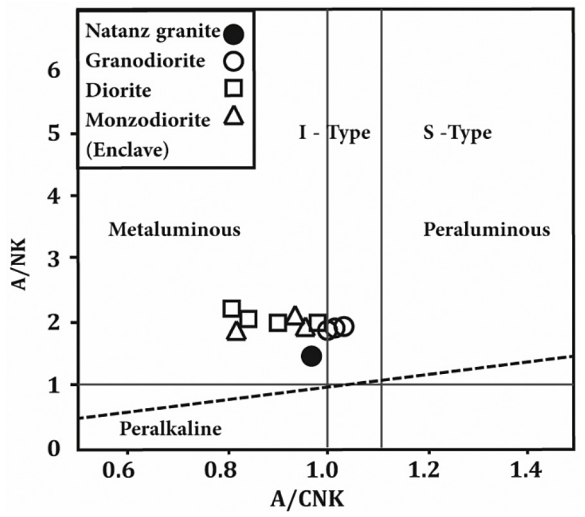

Fig. 6. Plot of the Golabad and Natanz granitoid complex on the A/NK molecular ratio versus A/CNK diagram (after Maniar and Piccoli, 1989) showed I-type metaluminous granitoid (Boundary between I- and S-type base on Chappell and White, 2001).

7. Discussion

7.1. Thermo-barometry

To estimate the temperature of the Golabad granitoid complex, chemical composition of plagioclases and biotites are used on the An-Ab-Or ternary diagram (Nekvasil et al., 2000), and it yielded the crystallization temperature and the pressure are in the range of 700–900 °C and 4.5 Kbar respectively (Fig. 10).

Patino Douce (1993) believes that temperature factor has a considerable influence on the solubility of Ti in biotite, therefore, the solubility of Ti is increased by increasing temperature. Thus, the Ti versus Mg/Mg + Fe diagram shows the biotites of the area with high Ti component (0.37–0.44) should be originated at high temperature (700–750 °C) (Fig. 11). Furthermore, when the whole rock analyses from the Natanz and Golabad granitoid complexes were plotted on the P_2O_5 versus SiO_2 diagram (Watson and Harrison, 1984) obtained the crystallization temperature ranges from 800 to 900 °C for both complexes (Fig. 12).

Since, the Al^{total} values in hornblende increases with pressure amounts, hence the values in magmatic hornblendes were used to determine the pressures of the studied granitoid rocks. The required conditions for the purpose are the presence of assemblage of quartz + plagioclase + K-feldspar + hornblende + biotite + titanite + magnetite + hematite. The pressure of the amphiboles crystallization from the Golabad granitoid complex was calculated base on Schmidt's (1992) study. Using geobarometry equation: $P\ (\pm 0.6\ Kbar) = 4.76\ Al^{Total} - 3.0$, the pressure of 1.29, 2.28 and 1.09 Kbar were obtained for the granodiorite, diorite and monzodiorite (enclaves) respectively. By using the equation of: $P = \rho gh$, and base on these data, the depth of emplacement of the Golabad granitoid complex should be 4.8, 8.6 and 4.1 Km (in order, for granodiorite, diorite and enclaves), corresponding to the high-level granitoids (Vernon, 1983).

As the pressure increases, more Al^{IV} replaces Fe and Mg in amphiboles, whereas, the increase of temperature caused the more replacement of Si with Al^{IV} (Hawthorne, 1981; Anderson and Smith, 1995). However, it must be noted that the amount of Al in amphibole is sensitive to crystallization environment conditions and the oxygen fugacity. Thus, when the fO_2 is less, more Fe^{2+} are incorporated into the amphibole framework and high Fe^{2+}/Fe^{3+} ratio caused the substitution of more Mg by Al (Stein and Dietl, 2001). The simultaneous presence of magnetite, titanite, and quartz with amphibole from the Golabad granitoid can be evidence of high oxygen fugacity in the parent magma. In view of Ewart (1979) magmas that are generated at the convergent edge are characterized by high oxygen fugacity. According to Anderson and Smith (1995), the amphiboles are suitable minerals to determine the oxygen fugacity, which are in range of Al^{IV}>0.75 and $Fe^{Total}/(Fe^{Total} + Mg) > 0.3$. Using $Fe^{Total}/(Fe^{Total} + Mg)$ versus Al^{IV} diagram (Anderson and Smith, 1995) all of the amphibole samples of the studied area were crystallized in high oxygen fugacity conditions (Fig. 13).

7.2. Tectonic setting

Mineral chemistry (i.e. biotite and amphibole) can be used to identify the tectonic setting and petrogenesis of the granitoid rocks (Maulana et al. 2012). Abdel Rahman (1994) believes that biotites can reflect the tectonic environment of host rocks. Thus, Al^{VI}, Ti^{4+} and Fe^{3+} content from biotites have significant role in distinguishing the petrogenesis of rocks (Buddington and Lindsley, 1964).

Abdel Rahman (1994) introduces three tectonic fields for various rock types: A) anorogenic extension-related alkaline rocks; P) peraluminous rocks including S-type granites and C) calc-alkaline I-type orogenic suites.

To distinguish tectonic setting of the studied area, the biotite data were plotted on Al_2O_3 versus MgO diagram (Abdel Rahman, 1994). It suggested that all of the samples related to the calc-alkaline,I-type orogenic magmas field (Fig. 14). Coltorti et al. (2007) expressed that the Na_2O and TiO_2 contents of the subduction related amphibole (S-Amph), are low in analogy to those of intra-plate amphibole (I-Amph). All the studied amphiboles are poor in Na_2O and TiO_2 contents and on Na_2O versus SiO_2 diagram, they all are clustered in S-Amph domain (Fig. 15). These results are consistent with the whole rocks geochemical analyses of the Golabad granitoid complex that carried out by Jahanbakhsh (2014).

In addition to mineral chemistry of some minerals, petrographic and geochemistry of special trace and rare earth elements can be used to distinguish the tectonic setting of the granitic rocks. All of the studied granitic rocks on Rb versus Y + Nb diagram (Pearce et al., 1984) are classified as volcanic arc granites (Fig. 16) and on

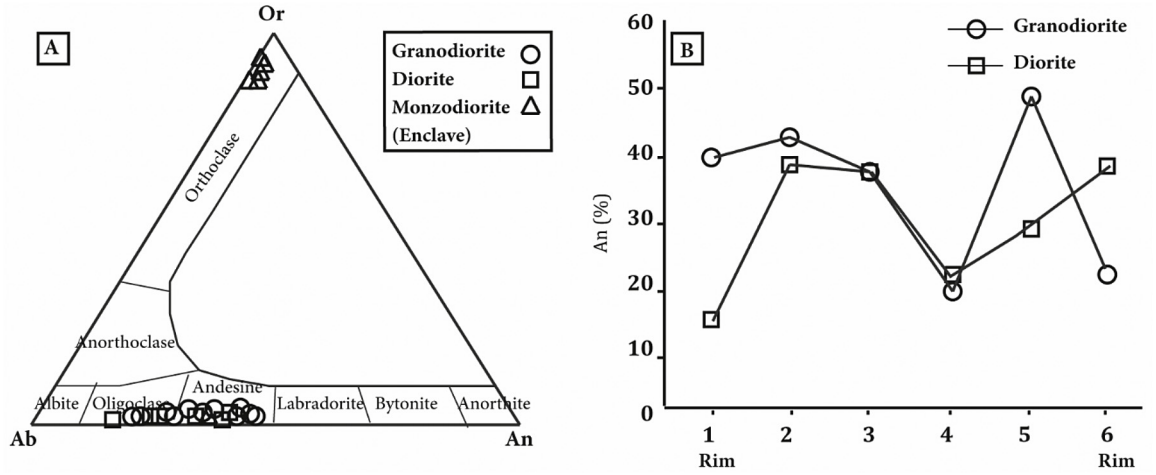

Fig. 7. Mineral chemistry of the plagioclase from the studied area. (A) Plot of the chemical data of the studied plagioclase on the Or-Ab-An triangle diagram (after Deer et al., 1992); (B) Oscillatory zoning of the studied plagioclases is a one of the evidence for magma mixing process.

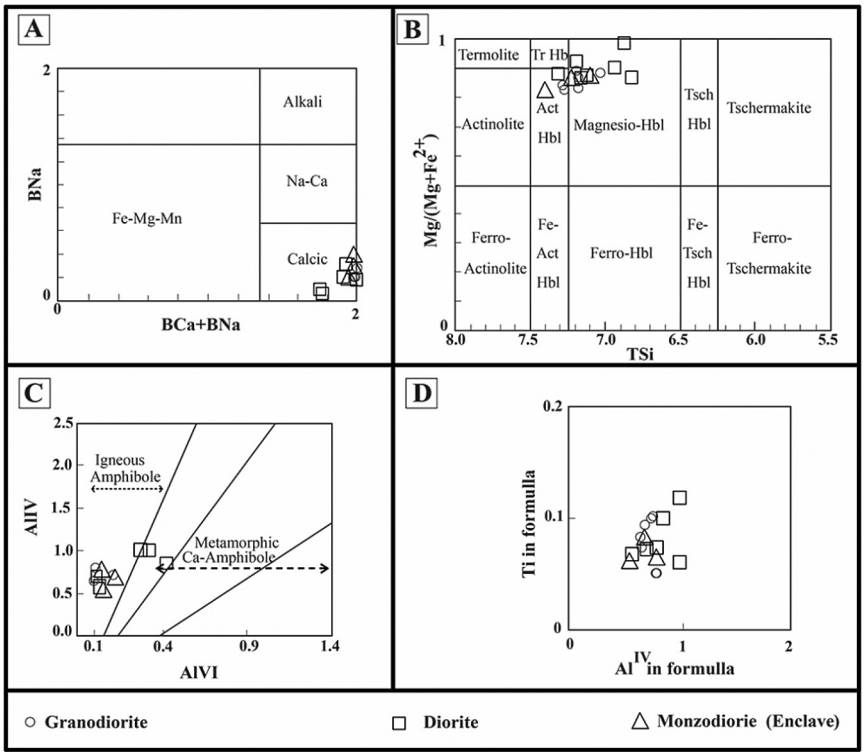

Fig. 8. The chemical composition of the amphiboles from the Golabad granitoid body: on (A) (B) BNa versus BCa + BNa and Mg/(Mg + Fe) versus TSi (Leake et al., 1997); (C) Al^{IV} versus Al^{VI} diagrams (after Fleet and Barnett, 1978); (D) Plot of amphibole data on Ti versus Al^{IV} diagram (after Leake et al., 1997).

La/Yb versus Th/Yb diagram (Condie, 1989) fall in the continental margin arc domain (Fig. 17). Didier and Barbarin (1991) and Gray and Kemp (2009) considered that calc-alkaline granitoids in related to volcanic arc are as continental arc hybrid granitoid. Also, they believe crustal and mantle sources are involved in generation of calc-alkaline granitoids. Granitoids can be created by partial melting of greywackes/igneous rocks (Patino Douce, 1999). The Golabad and Natanz granitoid samples are characterized by the high Na_2O values (2.98–4.63 wt%), low ASI values (0.80–1.02), K_2O/Na_2O ratios (0.39–0.95), Rb/Sr (0.07–0.28) and low range of Zr (63.5–154 ppm). On this account, it should be concluded that the rocks under discussion may be originated from partial melting of igneous rocks or high degree metamorphism. Moreover, by plotting the Golabad and Natanz granitoid complexes on the (Na_2O + K_2O)/(FeO + MgO + TiO_2) versus (Na_2O + K_2O + FeO + MgO + TiO_2) diagram (Patino Douce, 1999), it can be deduced that both complexes originated by partial melting of amphibolite source (Fig. 18).

The trace and rare earth elements patterns can explain the sources of igneous materials LREE enrichment relative to HREE on the chondrite normalizes REE pattern point to the presence of LREE rich minerals such as: plagioclase, zircon, titanite and apatite in melt (Fig. 19A) and the absence of HREE rich minerals including garnet and/or its remaining in the source as restite (Rollinson, 1993). On the other hand, it refers to the magma which formed

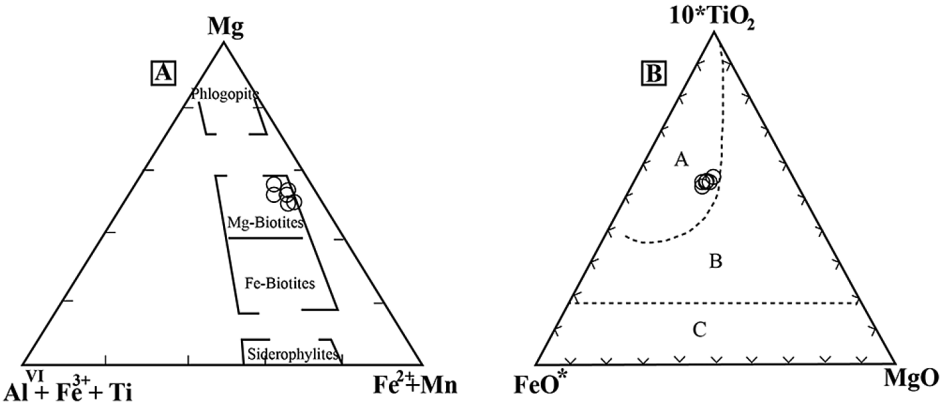

Fig. 9. Chemical compositions of the studied biotites on ternary diagrams: (A) Mg-(Fe^{2+}+Mn)-(Al^{VI} + Fe^{3+}+Ti) (after Foster, 1960); (B) 10*TiO_2-FeO*-MgO (after Nachit et al., 2005).

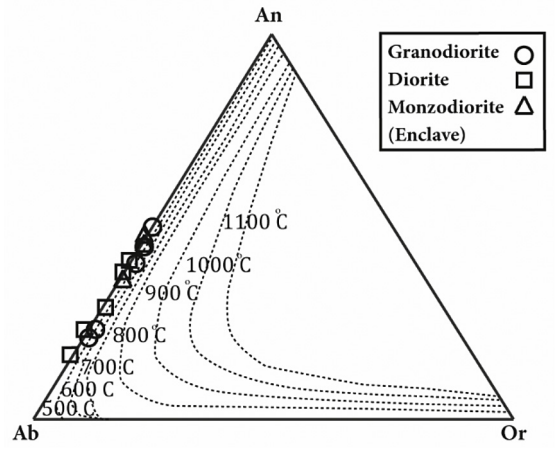

Fig. 10. Plot of the plagioclase data on An-Ab-Or ternary diagram (after Nekvasil et al., 2000), pointing to temperature of feldspar crystallization at a pressure of 4.5 Kbar range of 700–900 °C.

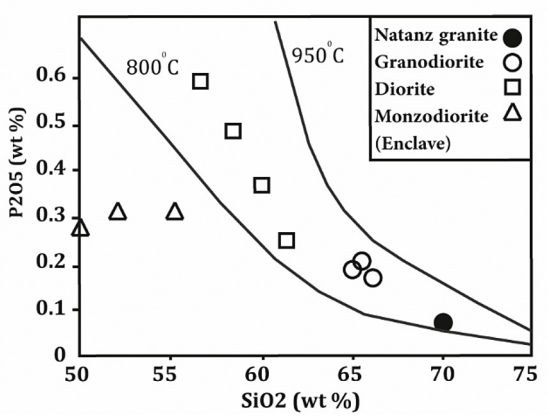

Fig. 12. Plot of the Golabad and Natanz granitoid rock analyzes on P_2O_5 versus SiO_2 diagram (after Watson and Harrison, 1984).

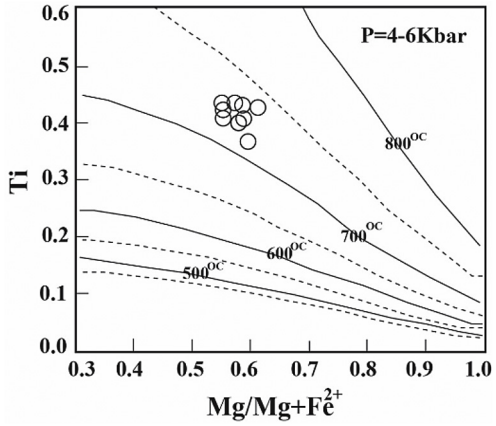

Fig. 11. Ti versus Mg/Mg + Fe diagram (after Henry et al., 2005), for biotite data from the area shows crystallization temperature ranges from 700 to 750 °C.

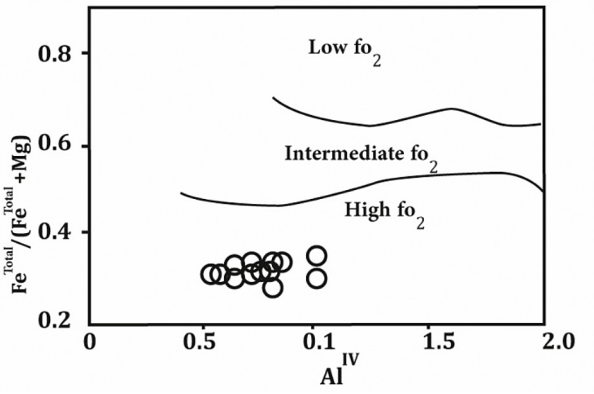

Fig. 13. The amphiboles from the studied area on $Fe^{Total}/(Fe^{Total} + Mg)$ versus Al^{IV} diagram (after Anderson and Smith, 1995) showed high oxygen fugacity conditions.

under depth of garnet stability field (Cotton et al., 1995). According to Rollinson (1993), this enrichment can be as a consequence of low degree of partial melting. The fair positive Eu anomaly (Eu/Eu* = 1.06–1.23) in the studied granodiorite and the diorite samples suggests the presence of the reduction conditions and crystallization of amphibole and zircon from the melt (Rollinson, 1993). While, one sample belonging to Oligo-Miocene granitoid Natanz (Honarmand et al., 2010) shows relatively negative anomaly (Eu/Eu* = 0.75). This feature can be as a result of feldspar differentiation from melt in high oxygen fugacity conditions. Primitive mantle normalized trace element patterns showed enrichment in LILE (e.i. Sr, Ba, K, Rb, Cs) and HFSE depletion (e.i. Nb, Ti) a remarkable feature related to magmas generated at the subduction zone (Rollinson, 1993; Yan and Zhao, 2008). LILE high

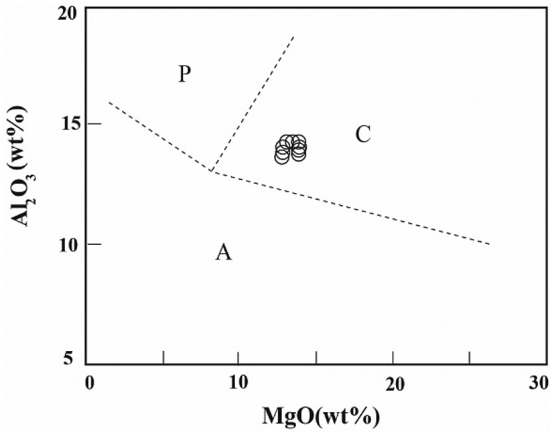

Fig. 14. All the biotite samples related to the calc-alkaline I-type orogenic magmas on Al_2O_3 versus MgO diagram (after Abdel Rahman, 1994).

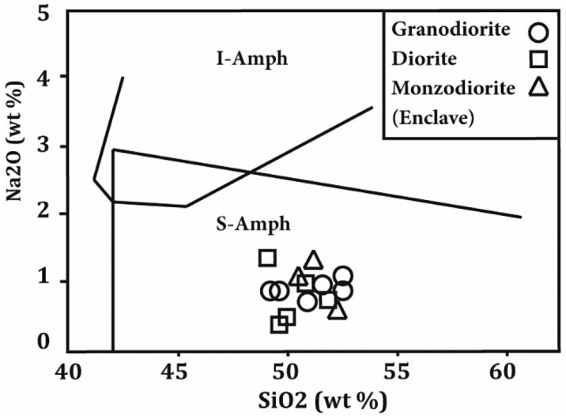

Fig. 15. On Na_2O versus SiO_2 diagram (after Coltorti et al., 2007) all amphibole samples fall on S-Amph domain.

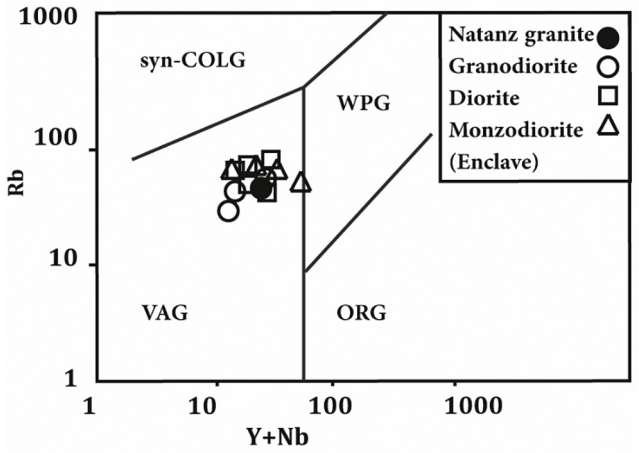

Fig. 16. The Golabad and Natanz granitoid rocks fall in the volcanic arc granitoid domain (after Pearce et al., 1984).

concentrations may also be due to subducted slab interference and contamination of mafic magma special with continental crust derived magma (Almeida et al., 2007) (Fig. 19B). Furthermore, the average of Th/U ratios of the studied samples (>2.5) are consistent with the upper continental crust composition (Taylor and

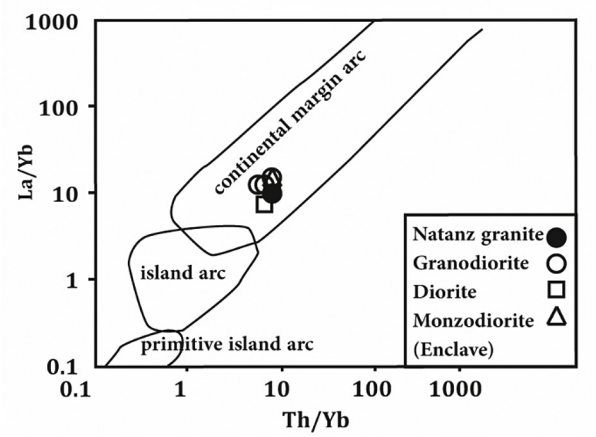

Fig. 17. Plot of the Golabad and Natanz granitoid rock samples on the La/Yb versus Th/Yb diagram (after Condie, 1989).

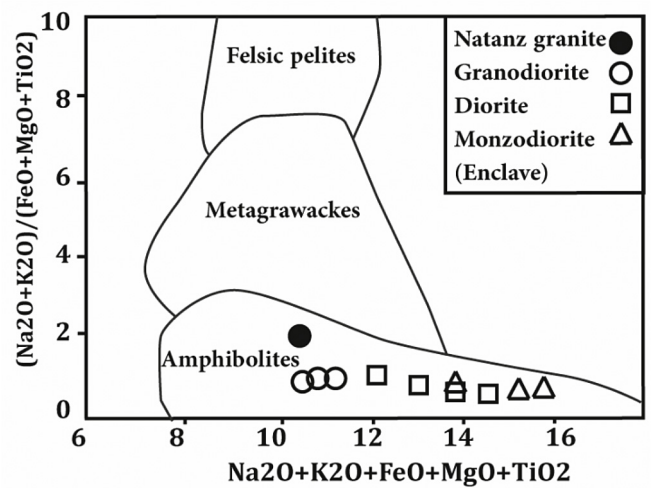

Fig. 18. All of the Golabad and Natanz granitoid rocks formed by partial melting of amphibolites (after Patino Douce, 1999).

McLennan, 1985). In order to distinguish the general geodynamic view of the Urumieh Dokhtar magmatic arc (UDMA) several Oligo-Miocene granitoid complexes were tried (Table 6). By comparison the thermo-barometer and their depth data, it seems that the Oligo-Miocene plutons in the central of the Urumieh Dokhtar were mostly emplaced at pressure of less than 3 Kbar and approximately 9 Km depth.

8. Conclusion

On the base of its field, mineralogical and chemical criteria, the Oligo-Miocene Golabad granitoid complex are dominated by diorite, granodiorite, granite, and monzodiorite (as enclaves). The complex represents medium to high-K calc-alkaline affinity with ASI = 0.80–1.02 value and metaluminous and I-type nature.

The plagioclases in the diorite and granodiorite as well as in the enclaves are oligoclase to andesine and the crystallization temperature ranges from 700 to 900 °C at pressure of 4.5 Kbar. Also, the studied biotites are classified as Mg-biotite and are primary phases, while the biotites from the enclaves are equilibrated primary phases. The biotites from the granodiorites due to having high Ti content (0.37–0.44), point to the formation crystallization temperature is from 700 to 750 °C.

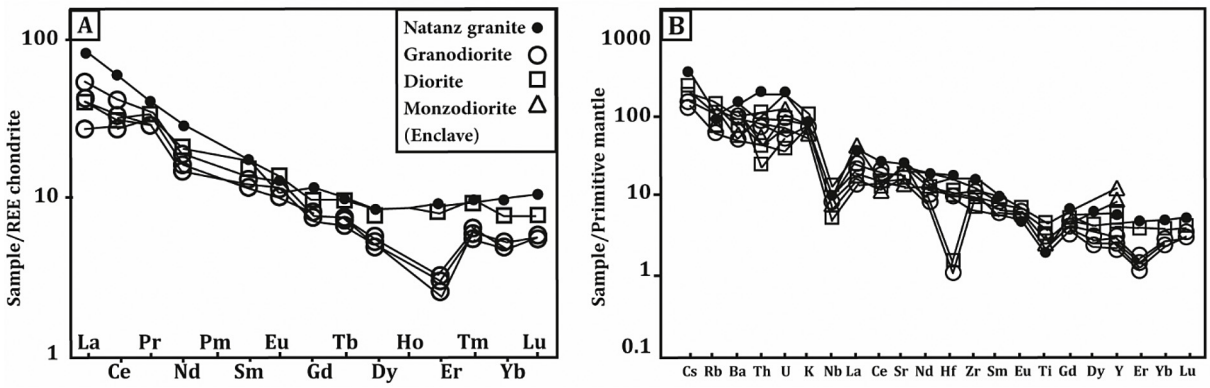

Fig. 19. (A) Chondrite-normalized REE patterns for the studied samples (values from Boynton, 1984), (B) Primitive mantle-normalized spider diagrams (based on data from Sun and McDonough, 1989).

Table 6
P-T and depth formation conditions of the several Oligo-Miocene granitoid complexes in UDMA to compare to the Golabad granitoid complex.

Plutonic complex	Calibration Method	Temperature (calibration by mineral)	Pressure (calibration by mineral)	Depth	Reference
Nabar pluton	Anderson and Smith (1995)	750 - 800 °C (amphibole-clinopyroxene)	2–2.15 Kbar (Al in amphibole)	7.5 –8.1 Km	Abbasi et al. (2014)
Niyasar granitoid complex	Anderson and Smith (1995)	706 - 756 °C (hornblende-plagioclase)	1-2 Kbar (Al in amphibole)	3.5 –7.5 Km	Honarmand et al. (2014)
Ghohroud Igneous complex	Putirka (2008)	1007 - 1158 °C (clinopyroxene)	2.3–4.4 Kbar (clinopyroxene)	8.6 –16.6 Km	Ghasemi and Tabatabaei Manesh (2015)
Natanz complex	Blundy and Holland (1990)- Anderson and Smith (1995)	705.15 °C (Hornblende-plagioclase)	2.27 Kbar (Al in amphibole)	8.5 Km	Honarmand et al. (2009)
Golabad granitoid complex	Schmidt (1992)	700-750 °C (Biotite)	1.09–2.28 Kbar (Al in amphibole)	4.1 –8.6 Km	This research

In general, the amphiboles are igneous phases, member of calcic group with magnesio-hornblende and actinolite-hornblende components an indicative of I- type nature of the Golabad granitoid complex that were possibly emplaced in subduction environment in an active continental margin. The hypothesis is supported by plotting the chemical analyses of the amphiboles on the Na_2O versus SiO_2 and TiO_2 versus SiO_2 diagrams. Moreover, the chemical biotite data from the area display that all of the samples related to the calc-alkaline I-type orogenic magmas field. The simultaneous presence of minerals such as: magnetite, titanite and quartz with amphibole can be taken as an evidence of high oxygen fugacity in the parent magma. P-T calculations according to amphibole barometry and plagioclase, biotite thermometry in accompany with the P_2O_5-SiO_2 diagram yielded the pressure from 1.09 to 2.28 Kbar and crystallization temperature ranges from 700 to 900 °C for the studied rocks. Using the calculated pressure values the estimated depth of crystallization of the rocks in question should range from 4 to 9 Km.

The overall mineralogical and geochemical data including the presence of apatite needle, dusty zone in plagioclase/with rounded shape, oscillatory zoning in the plagioclases, assemblages of the biotite flakes within the basalts as well as the existence of the mafic microgranular enclaves (MME) in the Golabad granitoid complex are indicative of magma mixing event. Furthermore, the amount of Al^{IV} (0.60–0.84) and Ti (0.04–0.09) in amphiboles supports the hypotheses.

The Golabad granitoid complex possibly developed during subduction of Neo-Tethys oceanic crust beneath the Central Iranian micro-continent during the Late Cretaceous–Early Tertiary time.

Acknowledgment

The authors are grateful to Iman Jahanbakhsh M.Sc. graduated student from Department of Geology, Isfahan University, Iran, for giving us the several analytical data from the study area. We wish to thank Dr. Shirin Fatahi for drawing and editing several diagrams. We are thankful to constructive reviewers from the Journal. The authors express the gratitude to the respected editor Dr. Read Brown Mthanganyika Mapeo which improved the original manuscript.

References

Abbasi, S., Tabatabaei Manesh, S.M., Karimi, S., Parfenova, O.V., 2014. Relative contributions of crust and mantle to generation of Oligo-Miocene medium-K calc-alcaline I –type granitoids in a subduction setting- a case study from the Nabar pluton, Central Iran. Petrol. Springer 22 (3), 310–328.
Abdel Rahman, A., 1994. Nature of biotite from alkaline, calc-alkaline, and per-aluminous magmas. J. Petrol. 35, 525–541.
Alavi, M., 1994. Tectonics of the zagros orogenic belt of Iran: new data and interpretations. Tectonophysics 229, 211–238.
Alavi, M., 2004. Regional stratigraphy of the Zagros Fold-Thrust Belt of Iran and its proforeland evolution. Am. J. Sci. 304, 1–20.
Almeida, M.E., Macambira, M.J.B., Oliveira, E.C., 2007. Geochemistry and zircon geochronology of the I-type high-K calc-alkaline and S-type granitoid rocks from Southeastern Roraima, Brazil: Orosirian collisional magmatism evidence (1.97–1.96 Ga) in central portion of Guyana Shield. Precambrian Res. 155, 69–97.
Amidi, S.M., 1975. Contribution àlétude stratigraphique, pétrologique et pétrochimique des roches magmatiques de la région Natanz-Nain-Surk (Iran

Central). Unpublished PhD Thesis, Grenoble.
Amidi, S.M., Alavi, M., 1978. Geological Map of the Nain Quadrangle 1, 250000 No. G8. Geological Survey of Iran.
Anderson, J.L., Smith, D.R., 1995. The effects of temperature and fO_2 on the Al-in-hornblende barometer. Am. Mineral. 80, 549–559.
Barbarin, B., 2005. Mafic magmatic enclaves and mafic rocks associated with some granitoids of the central Sierra Nevada batholiths, California: nature, origin, and relations with the hosts. Lithos 80, 155–177.
Berberian, F., Berberian, M., 1981. Tectono-plutonic episodes in Iran. In: Delany, F.M., Gupta, H.K. (Eds.), Zagros, Hindu Kush, Himalaya Geodynamic Evolution American Geophysical Union Geodynamics Series, vol. 3, pp. 5–27.
Best, M.G., 2003. Igneous and Metamorphic Petrology. Wiley-Blackwell, England, p. 752.
Blundy, J.d., Holland, t.J.B., 1990. Calcic amphibole equilibria and a new amphibole-plagioclase geothermometer. Contrib. Mineral. Petrol. 104, 208–224.
Boynton, W.V., 1984. Cosmochemistry of the rare earth elements, meteorite studies. In: Henderson, P. (Ed.), Rare Earth Element Geochemistry, Developments in Geochemistry. Elsevier, Amsterdam, pp. 63–114.
Buddington, A.F., Lindsley, D.H., 1964. Iron- titanium oxide minerals and synthetic equivalents. J. Petrol. 54, 310–357.
Chappell, B.W., White, A.J.R., 2001. Two contrasting granite types, 25 years later. Aust. J. Earth Sci. 48, 489–499.
Coltorti, M., Bonadiman, C., Faccini, B., Gregoire, M., O'Reilly, S.Y., Powell, W., 2007. Amphiboles from suprasubduction and intraplate lithospheric mantle. Lithos 99, 68–84.
Condie, K.C., 1989. Geochemical changes in basalts and andesites across the Archean-Proterozoic boundary: identification and significance. Lithos 23, 1–18.
Cotton, J., Le Dez, A., Bau, M., Caroff, M., Maury, R.C., Dulski, P., Fourcade, S., Bohn, M., Brousse, R., 1995. Origin of anomalous rare earth element and yttrium enrichments in subaerially exposed basalts, evidence from French Polynesia. Chem. Geol. 119, 115–138.
Deer, W.A., Howie, R.A., Zussman, J., 1992. An Introduction to the Rock Forming Minerals. Longman, London, p. 692.
Didier, J., 1973. Granites and Their Enclaves, the Bearing of Enclaves on the Origin of Granites. Elsevier, Amsterdam, p. 393.
Didier, J., Barbarin, B., 1991. Enclaves and Granite Petrology. Developments in Petrology. Elsevier, Amsterdam, p. 525.
Emami, M.H., 1981. Ge'ologie de la re'gion de Qom-Aran (Iran): contribution a l'e'tude dynamique et ge'ochimique du volcanisme Tertiaire de l'Iran Central. Unpublished PhD Thesis. University of Grenoble, France.
Ewart, A., 1979. A review of the mineralogy and chemistry of Tertiary recent dacitic, latitic, rhyolitic and related salic volcanic rocks. In: Fred, B. (Ed.), Trondhjemites, Dacites, and Related Rocks. Springer, Verlag Berlin, pp. 12–101.
Finch, A.A., Parsons, I., Mingard, S.C., 1995. Biotites as indicators of fluorine fugacities in late-stage magmatic flu-ids: the Gardar province of south Greenland. J. Petrol. 36, 1701–1728.
Fleet, M.E., Barnett, R.L., 1978. Partitioning in calciferous amphiboles from the Frood Mine, Sudbury, Ontario. Can. Mineral. 16, 527–532.
Foster, M.D., 1960. Interpretation of the Composition of Trioctahedral Micas, 354 B. US Geological Survey, pp. 11–49. Professional Paper.
Ghasemi, A., Tabatabaei Manesh, S.M., 2015. Geochemistry and petrogenesis of Ghohroud igneous complex (Urumieh Dokhtar zone); evidence for Neotethyan subduction during the Neogene. Arab. J. Geosci. 8, 9599–9623.
Ghasemi, A., Talbot, C.J., 2006. A new tectonics cenario for the Sanandaj–Sirjan Zone (Iran). J. Asian Earth Sci. 26, 683–693.
Gray, C.M., Kemp, A.I.S., 2009. The two-component model for the genesis of granitic rocks in southeastern Australia—nature of the metasedimentary-derived and basaltic end members. Lithos 111, 113–124.
Hattory, K., Sato, H., 1996. Magma evolution recorded and plagioclase zoning in 1991 pinatubo eruption products. Am. Mineral. 88, 982–984.
Hawthorne, F.C., 1981. Crystal chemistry of the amphiboles. Mineral. Soc. Am. Rev. Mineral. 9A, 1–102.
Henry, D.J., Guidotti, C.V., Thomson, J.A., 2005. The Ti-saturation surface for low-to-medium pressure metapelitic biotite: implications for Geothermometry and Ti-substitution Mechanisms. Am. Mineral. 90, 316–328.
Honarmand, M., Moayyed, M., Jahangiri1, A., Ahmadian, J., 2009. Mineralogy, geothermobarometry and magmatic series of Natanz plutonic complex. Iran. Soc. Crystallogr. Mineral. 17 (3), 325–342.
Honarmand, M., Moayyed, M., Jahangiri, A., Ahmadian, J., Bahadoran, N., 2010. The study of geochemical characteristics of Natanz plutonic complex, North of Isfahan. Petrology 3 (1), 65–89 (In Persian).
Honarmand, M., Rashidnejad Omran, N., Neubauer, F., Hashem Emami, M., Nabatian, G., Liu, X., Dong, Y., von Quadt, A., Chen, B., 2014. Laser-ICP-MS U-Pb zircon ages and geochemical and Sr-Nd-Pb isotopic compositions of the Niyasar plutonic complex, Iran: constraints on petrogenesis and tectonic evolution. Int. Geol. Rev. 56, 104–132.
Jahanbakhsh, I., 2014. Petrology of the Gojed Intrusive Mass and Volcanic Rocks (East of Isfahan). Unpublished M.Sc.. Thesis Isfahan University, Iran (In Persian).
Javanmardi, M., Davoudian, A., 2009. Study of basalts in south of Asad Abad (north-east of Koohpayeh, Isfahan Province) with reference to very low-grade metamorphism of these rocks. Iran. J. Crystallogr. Mineral. 17 (1), 29–42 (In Persian).
Kazmin, V.G., Sbortshikov, I.M., Ricou, L.E., Zonenshain, L.P., Boulin, J., Knipper, A.L., 1986. Volcanic belts as markers of the Mezozoic-Cenozoic active margin of Eurasia. Tectonophysics 123 (1–4), 123–152.
Leake, B.E., Wolley, A.R., Arps, C.E.S., Birch, W.D., Gilbert, M.C., Grice, J.D., Hawthorne, F.C., Kato, A., Kisch, H.J., Krivovichev, V.G., Linthout, K., Laird, J., Mandarino, J., Maresch, W.V., Nickel, E.H., Rock, N.M.S., Schumacher, J.C., Smith, D.C., Stephenson, N.C.N., Ungaretti, L., whittaker, E.J.W., Youzhi, G., 1997. Nomenclature of Amphiboles, report of the subcommittee on amphiboles of the international mineralogical association commission on new minerals and mineral names. Can. Mineral. 35 (1), 219–246.
Maniar, P.D., Piccoli, P.M., 1989. Tectonic discrimination of granitoids. Geol. Soc. Am. Bull. 101, 635–643.
Mansouri Esfahani, M., Norbehesht, I., 1997. Petrology of Gojed intrusive and associated volcanic. Geosciences 23–24, 79–94 (In Persian).
Maulana, A., Watanabe, K., Imai, A., Yonezu, K., 2012. Geochemical signature of granitic rocks from Sulawesi, Indonesia: evidence of Gondwana involvement. Mineral. Mag. 76, 2081.
Middlemost, E.A.K., 1994. Naming materials in the magma igneous rock system. Earth Sci. Rev. 37, 215–224.
Nachit, H., Ibhi, A., Abia, E.H., Ohoud, M.B., 2005. Discrimination between primary magmatic biotites, re-equilibrated biotites and neo-formed biotites: geomaterials (Mineralogy). Compt. Rendus Geosci. 337, 1415–1420.
Nekvasil, H., Simon, A., Lindsley, H., 2000. Crystal fractionation and the evolution of intra-plate hy-normative igneous suites: insights from their feldspar. J. Petrol. 41 (12), 1743–1757.
Patino Douce, A.E., 1993. Titanium substitution in biotite: an empirical model with applications to thermometry, O_2 and H_2O barometries, and consequences from biotite stability. Chem. Geol. 108, 133–162.
Patino Douce, A.E., 1999. What do experiments tell us about the relative contributions of crust and mantle to the origins of granitic magmas?. In: Castro, A., Fernandez, C., Vigneresse, J.L. (Eds.), Understanding Granites: Intergrating New and Classical Techniques, vol. 168. Geological Society of London, Special Publication, pp. 55–75.
Pearce, J.A., Harris, N.B., Tindle, A.G., 1984. Trace element discrimination diagrams for the tectonic interpretation of granitic rocks. J. Petrol. 25, 956–983.
Peccerillo, A., Taylor, S.R., 1976. Geochemistry of Eocene calc-alkaline volcanic rocks from the Kastamonu area, Northern Turkey. Contrib. Mineral. Petrol. 58, 63–81.
Putirka, K., 2008. Thermometers and barometers for volcanic systems. Rev. Mineral. Geochem. 69, 61–120.
Rollinson, H.R., 1993. Using Geological Data, Evolution, Presentation, Interpretation. Longman, Scientific and Technical, London.
Richards, J.P., Sholeh, A., 2016. The Tethyan tectonic history and Cu-Au metallogeny of Iran. Soc. Econ. Geol. Spec. Publ. 19, 193–212.
Sabzehei, M., 1994. Geological Quadrangle Map of Iran. No. 12, Hajiabad, 1:250,000, First compilation by Berberian, M., final compilation and revision by Sabzehei, M.. Geological Survey of Iran.
Schmidt, W.S., 1992. Amphibole composition in tonalite a function of pressure: an experimental calibration of the Al-in-hornblende barometer. Contrib. Mineral. Petrol. 110, 304–310.
Shelley, D., 1993. Igneous and Metamorphic Rocks under the Microscope. Chapman and Hall, London.
Stein, E., Dietl, C., 2001. Hornblende thermobarometry of granitoids from the Central Odenwald (Germany) and their implications for the geotectonic development of the Odenwald. Mineral. Petrol. 72, 185–207.
Sun, S.S., McDonough, W.F., 1989. Chemical and isotopic systematics of oceanic basalts: implications for mantle composition and processes, magmatism in ocean basins. J. Geol. Soc. Lond. Specific Pub. 42, 313–345.
Taylor, S.R., McLennan, S.M., 1985. The Continental Crust: Its Composition and Evolution. Blackwell Scientific Publication, Carlton, p. 312.
Torabi, G., 2009. Subduction-related Eocene Shoshonites from the Cenozoic Urumieh-Dokhtar Magmatic Arc (Qaleh-Khargooshi Area, Western Yazd Province, Iran). Turk. J. Earth Sci. 18, 583–613.
Vernon, R.H., 1990. Crystallization and hybridism in microgranitoid enclave magmas: microstructural evidence. J. Geophys. Res. 95, 17849–17859.
Vernon, R.H., 1983. Restite, xenoliths and microgranitoid enclaves in granites (Clarke Memorial Lecture). J. Proc. Roy. Soc. N. S. W. 116 (1), 77–103.
Watson, E.B., Harrison, T.M., 1984. Accessory minerals and the geochemical evolution of crustal magmatic systems a summary and prospectus of experimental approaches. Phys. Earth Planet. In. 35, 10–30.
Whitney, D.L., Evans, B.W., 2010. Abbreviations for names of rock-forming minerals. Am. Mineral. 95, 185–187.
Wones, D.R., 1989. Significance of the assemblage titanite + magnetite + quartz in granitic rocks. Am. Mineral. 74 (7–4), 744–749.
Wones, D.R., Eugster, H.P., 1965. Stability of biotite: experiment, theory and application. Am. Mineral. 50 (9), 1228–1272.
Yan, J., Zhao, J.X., 2008. Cenozoic alkali basalts from Jingpohu, NE China, The role of lithosphere asthenosphere interaction. J. Asian Earth Sci. 33, 106–121.
Zorpi, M.J., Coulon, C., Orisini, J.B., Concirta, C., 1989. Magma mingling, zoning and emplacement in calk-alkaline granitoid plutons. Tectonophysics 157, 315–326.